Cancer Cell
Article

S1PR1-STAT3 Signaling Is Crucial for Myeloid Cell Colonization at Future Metastatic Sites

Jiehui Deng,[1] Yong Liu,[1] Heehyoung Lee,[1] Andreas Herrmann,[1] Wang Zhang,[1] Chunyan Zhang,[1] Shudan Shen,[1] Saul J. Priceman,[1] Maciej Kujawski,[1] Sumanta K. Pal,[2] Andrew Raubitschek,[1] Dave S.B. Hoon,[5] Stephen Forman,[3] Robert A. Figlin,[6] Jie Liu,[7,8] Richard Jove,[4] and Hua Yu[1,8,*]
[1]Department of Cancer Immunotherapeutics and Tumor Immunology
[2]Department of Medical Oncology
[3]Department of Hematology and Hematopoietic Cell Transplantation
[4]Department of Molecular Medicine
Beckman Research Institute and City of Hope Comprehensive Cancer Center, Duarte, CA 91010, USA
[5]Department of Molecular Oncology, John Wayne Cancer Institute, Santa Monica, CA 90404, USA
[6]Department of Hematology-Oncology, Cedars-Sinai Medical Center, Los Angeles, CA 90048, USA
[7]Department of Digestive Diseases of Huashan Hospital, Department of Immunology of Shanghai Medical School, Fudan University, Shanghai, 200040, China
[8]Center for Translational Medicine, Zhangjiang High-Tech Park, Shanghai, 201203, China
*Correspondence: hyu@coh.org
DOI 10.1016/j.ccr.2012.03.039

SUMMARY

Recent studies underscore the importance of myeloid cells in rendering distant organs hospitable for disseminating tumor cells to colonize. However, what enables myeloid cells to have an apparently superior capacity to colonize distant organs is unclear. Here, we show that S1PR1-STAT3 upregulation in tumor cells induces factors that activate S1PR1-STAT3 in various cells in premetastatic sites, leading to premetastatic niche formation. Targeting either S1PR1 or STAT3 in myeloid cells disrupts existing premetastatic niches. S1PR1-STAT3 pathway enables myeloid cells to intravasate, prime the distant organ microenvironment and mediate sustained proliferation and survival of their own and other stromal cells at future metastatic sites. Analyzing tumor-free lymph nodes from cancer patients shows elevated myeloid infiltrates, STAT3 activity, and increased survival signal.

INTRODUCTION

Several seminal studies have documented the importance of myeloid cells in providing a sanctuary for tumor cells to adhere, survive, and colonize secondary sites (Erler et al., 2009; Hiratsuka et al., 2006; Kaplan et al., 2005; Kim et al., 2009; Kowanetz et al., 2010; Psaila and Lyden, 2009). Although myeloid cells are mobile and produce chemokines and other molecules in response to the tumor environment thereby promoting cancer progression (Biswas and Mantovani, 2010; Coussens et al., 2000; Du et al., 2008; Fan and Malik, 2003; Mantovani et al., 2008; Pollard, 2004; Shojaei et al., 2007), myeloid cells need to proliferate and evade apoptosis in order to establish colonies at future metastatic sites. However, mechanisms that enable myeloid cells to colonize in the hostile environment at future metastatic sites remain to be identified. In addition, the underlying molecular mechanism(s) that orchestrates tumor cells, myeloid cells, resident fibroblasts, and other stromal cell types to achieve outgrowths prior to tumor cell arrival at distant organs remains unknown. A more complete body of knowledge on such molecular mechanisms may facilitate translation of potentially paradigm-shifting therapeutic strategies for the treatment of

Significance

Conceptually, our results introduce the idea that S1PR1-STAT3 signaling axis is elevated in distant organs prior to tumor cell arrival, which empowers myeloid cells to invade, proliferate and resist apoptosis at premetastatic sites. We further identify a role of myeloid cells in regulating fibroblasts by producing factors similar to those of tumor cells, thereby facilitating formation of premetastatic niches. Additionally, we demonstrate the ability of STAT3 in regulating numerous genes crucial for premetastatic niche formation in bone marrow-derived cells. Perhaps the most significant aspect of our current studies is the therapeutic potential to target the S1PR1-STAT3 signaling axis to eliminate and/or reduce preformed premetastatic niches, thereby preventing tumor metastasis.

tumor metastasis: target premetastatic niches before clinical detection of metastasis.

Persistently activated STAT3 in tumor cells acting as a crucial oncogenic mediator and potent transcriptional factor has been widely documented (Bollrath et al., 2009; Bromberg et al., 1999; Catlett-Falcone et al., 1999; Chiarle et al., 2005; Fukuda et al., 2011; Grivennikov et al., 2009; Lee et al., 2010; Lesina et al., 2011; Yu et al., 2007, 2009). Recent studies have also demonstrated persistent activation of STAT3 in myeloid cells and T cells at primary tumor sites, promoting immunosuppression, tumor angiogenesis, tumor growth, and metastasis (Biswas and Mantovani, 2010; Kortylewski et al., 2005, 2009c; Kujawski et al., 2008; Wang et al., 2009). While many cytokines, chemokines, and growth factors can activate STAT3 in tumor cells and in tumor-associated stromal cells (Biswas and Mantovani, 2010; Bollrath et al., 2009; Catlett-Falcone et al., 1999; Grivennikov et al., 2009; Kortylewski et al., 2009c; Kujawski et al., 2008; Lee et al., 2010; Lesina et al., 2011; Wang et al., 2009; Yu et al., 2007), our recent studies showed a critical role of S1PR1 in maintaining persistent STAT3 activation in primary tumors, by regulating both tumor cells and tumor-infiltrating myeloid cells (Lee et al., 2010). S1PR1 and its ligand, S1P, play a fundamental role in endothelial cells for regulating tumor angiogenesis, which is also crucial for metastasis (Chae et al., 2004; Gao et al., 2008; Holmgren et al., 1995; Spiegel and Milstien, 2003; Visentin et al., 2006). Although the importance of tumor-infiltrating myeloid cells in facilitating tumor cell invasion and metastasis is well established, the role of myeloid cells in forming a sanctuary for tumor cells in distant organs prior to tumor cell arrival/outgrowth has only begun to be appreciated (Erler et al., 2009; Kaplan et al., 2005; Psaila and Lyden, 2009). Our current study investigates whether STAT3 is persistently activated at future metastatic sites prior to tumor cell arrival and whether S1PR1-STAT3 signaling in both tumor cells and myeloid cells is critical for tumor cell outgrowth/metastasis, and thus a potential therapeutic target.

RESULTS

S1PR1-STAT3-Induced Tumor Factors Activate S1PR1-STAT3 at Distant Premetastatic Sites

To investigate whether increased STAT3 signaling in tumor cells would induce production of factors that could prime distant premetastatic sites, we generated tumor conditioned media (TCM) from control or *S1pr1* overexpressing (*S1pr1*^{high}) mouse B16 melanoma and MB49 bladder tumor cells. The parental tumor cells display relatively low Stat3 activation in cultured cells, which was elevated by *S1pr1* overexpression (Lee et al., 2010). We examined several factors known to activate Stat3, and detected elevated levels of both IL-6 and IL-10 in the TCM derived from the *S1pr1*^{high} tumor cells (Figure S1A available online). We treated mice with TCMs from control and *S1pr1*^{high} tumor cells for 5 days prior to parental tumor cell challenge. Three days after tumor challenge when there were no detectable metastases, we observed extensive CD11b^{+} myeloid cell cluster formation in the lung (Figure 1A). Importantly, we also observed widespread Stat3 activation in lung-associated stromal cells by tumor-secreted factors (Figures S1B and S1C). Further analyses of CD11b^{+} myeloid cells indicated that changing Stat3 activity in tumor cells altered the number of myeloid-derived suppressor cells (Figure S1D).

We next performed experiments to ensure that in the absence of tumor cell challenge, treatment with TCM derived from *S1pr1*^{high} tumor cells could activate Stat3 in future metastatic sites and induce premetastatic niche formation in distant future metastatic sites. Our results showed that treating mice with the TCM from *S1pr1*^{high} tumor cells for 5 days could induce strong Stat3 activation and myeloid infiltration without tumor cell challenge (Figure 1B). Stat3 activity was detectable in myeloid cells and also widespread in the lung (Figure 1B). Furthermore, treating mice with TCM generated from *S1pr1*^{high} tumor cells, but not TCM derived from control tumor cells, was able to induce S1pr1 expression and phosphorylated Stat3 (p-Stat3) in both lung CD11b^{+} myeloid cells and metastatic nodules, which was accompanied by extensive metastasis at days 9 and 14 post-tumor cell challenge (Figure 1C). We also observed an increase in total Stat3 protein level, which is likely caused by autoregulation of p-Stat3.

Since resident fibroblasts at future metastatic sites play an important role in premetastatic niche formation (Kaplan et al., 2005; Orimo et al., 2005), and because we detected extensive Stat3 activation at the future metastatic sites (Figures 1A and 1B), we tested whether S1pr1-Stat3-induced tumor factors could activate fibroblasts to produce fibronectin, a factor crucial for premetastatic niche formation (Erler et al., 2009; Kaplan et al., 2005; Psaila and Lyden, 2009). Treating mouse embryonic fibroblasts (MEFs), as well as primary fibroblasts derived from mouse lungs, with TCM prepared from *S1pr1*^{high} tumor cells, but not that from control tumor cells, induced fibronectin expression and Stat3 activation (Figure 1D). Trypsin treatment of TCM for *S1pr1*^{high} tumor cells blocked fibronectin and Stat3 activation in the fibroblasts. Heat treatment of the same TCM also, to a lesser degree, reduced p-Stat3 level (Figure S1E).

Myeloid Cell S1PR1-STAT3 Is Crucial for Premetastatic Niche Formation

Since S1PR1-STAT3 signaling is activated at premetastatic sites and in myeloid clusters, we assessed whether Stat3 activation intrinsic to myeloid cells is required for maintaining S1pr1-Stat3 activity in the premetastatic sites and for formation of premetastatic niches. We induced *Stat3* ablation in the myeloid compartment with poly(I:C) treatment using *Mx1Cre-Stat3*$^{loxp/loxp}$ mice. Relative to the control *Stat3*$^{loxp/loxp}$ mice with intact *Stat3* alleles, ablating *Stat3* in the myeloid compartment of *Mx1Cre-Stat3*$^{loxp/loxp}$ mice effectively reduced Stat3 activity in the entire lung and eliminated formation of premetastatic niches (Figure 2A), as well as lung metastasis (Figure 2B, upper panel). In addition to CD11b^{+} cells, endothelial cells and fibroblasts were among the p-Stat3-positive cells, which were reduced by ablating *Stat3* in the myeloid compartment (Figure 2B, lower panel).

In vivo ablating *S1pr1* in myeloid cells using *Mx1Cre-S1pr1*$^{loxp/loxp}$ mice reduced Stat3 activity and myeloid clusters in the lung (Figure 2C). Additionally, increased *S1pr1* expression in tumor cells led to production of factors that elevated S1pr1 and p-Stat3 levels in the lungs, which required myeloid cell-specific S1pr1 expression (Figure S2A). The reduction in S1pr1

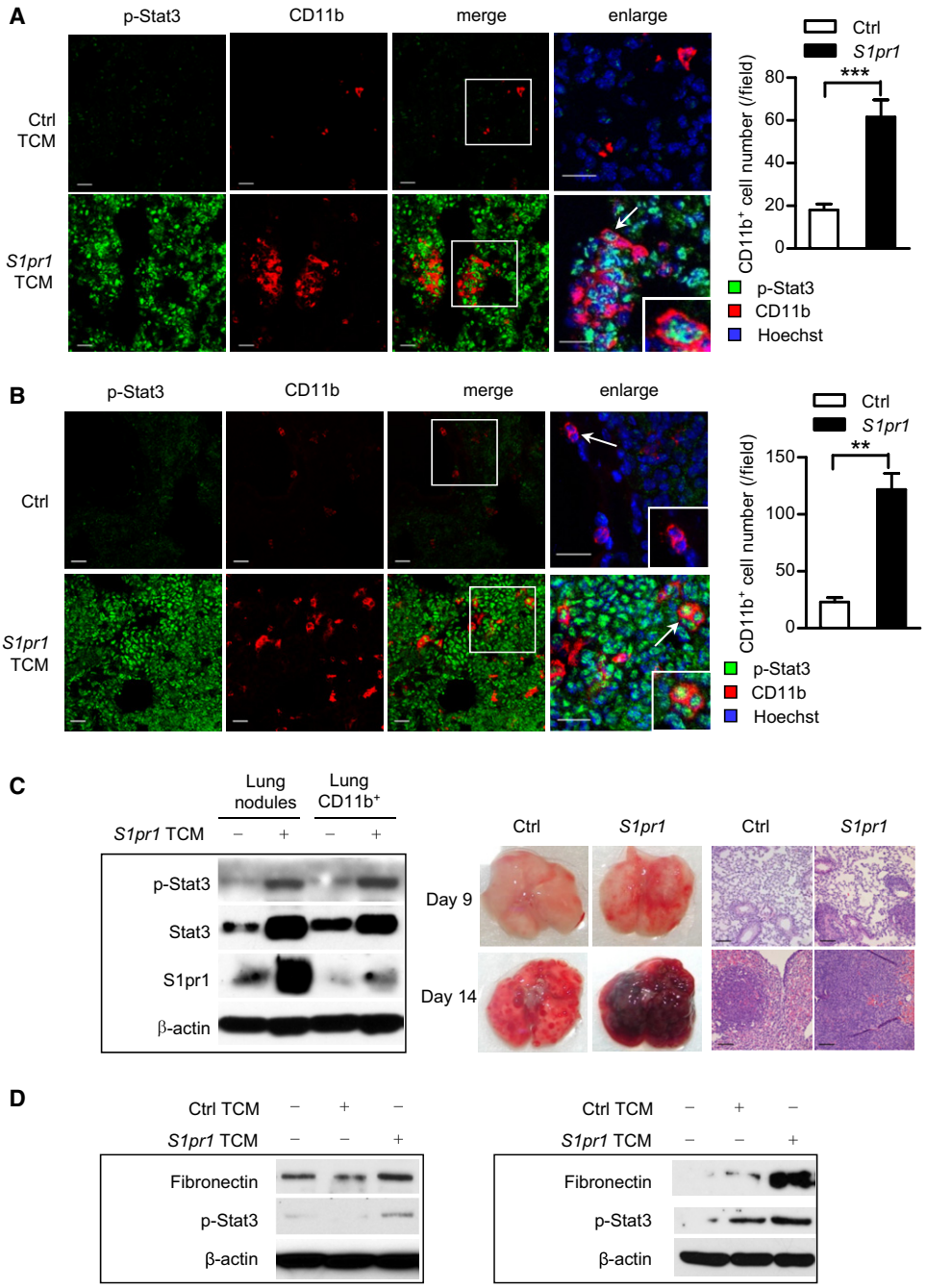

Figure 1. S1PR1-STAT3-Induced Tumor Factors Activate STAT3 at Premetastatic Sites

(A) Left: Confocal microscopy images show phospho-Stat3 (p-Stat3, green) in myeloid cell clusters (CD11b, red) and other cells in premetastatic lung tissue sections from mice treated with TCMs from control or *S1pr1* overexpressing tumor cells for 5 days, followed by systemic tumor challenge for 3 days. Scale bars, 20 μm. Right, quantification of infiltrating $CD11b^+$ cells shown on left (n = 10).

(B) Immunofluorescence (IF) staining measuring p-Stat3 and CD11b in lung sections from naive mice (upper panel) and mice treated with TCM from $S1pr1^{high}$ MB49 tumor cells for 5 days without tumor challenge (lower panel). Left: representative confocal images from 4 mice per group. Right, quantification of infiltrating $CD11b^+$ cells. Scale bars, 20 μm.

(C) Left panel, western blotting showing S1pr1, Stat3, and p-Stat3 in lung $CD11b^+$ myeloid cells and metastatic nodules in mice 14 days post-tumor injection. Right panel, representative lung metastasis and H&E staining (n = 6). Scale bars, 100 μm.

(D) Western blotting showing expression levels of fibronectin and p-Stat3 in MEFs (left) and primary lung-derived fibroblasts (right) exposed to indicated media. Results represent means ± SEM. $^{**}p < 0.01$, $^{***}p < 0.001$.

See also Figure S1.

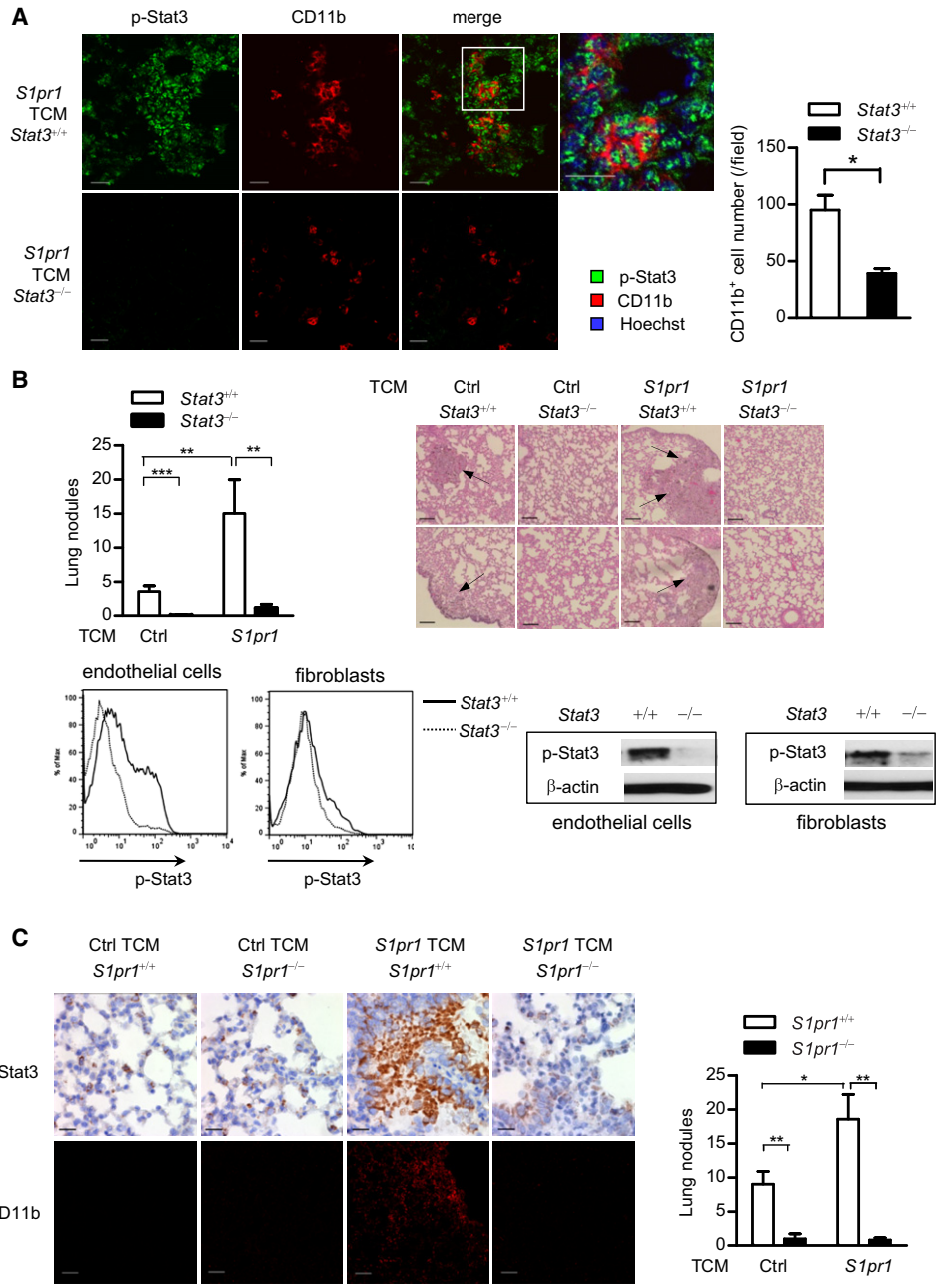

Figure 2. Ablating *S1pr1* or *Stat3* in Myeloid Cells Abrogates Tumor Factor-Induced Premetastatic Niches

(A) Representative immunofluorescence staining and confocal microscopy of p-Stat3 and CD11b$^+$ myeloid cells in lung tissues harvested from mice with *Stat3*$^{+/+}$ and *Stat3*$^{-/-}$ myeloid compartment. Right, quantification of the images (n = 9). Scale bars, 20 μm.

(B) Upper left panel, enumeration of metastatic lung nodules in mice with *Stat3*$^{+/+}$ and *Stat3*$^{-/-}$ myeloid compartment treated with indicated TCMs followed by parental tumor cell challenge (n = 9). Upper right panel, H&E staining shows histology of lungs from representative mice in each group, arrows indicate lung metastasis. Scale bars, 100 μm. Lower panel, flow cytometric analysis and western blotting measuring p-Stat3 in endothelial cells (CD31$^+$αSMA$^-$) and fibroblasts (CD31$^-$αSMA$^+$) in premetastatic sites.

(C) Mice were treated with indicated TCMs, followed by systemic parental tumor cell challenge. Left upper panel, IHC staining evaluates p-Stat3 expression in lung tissues from mice with *S1pr1*$^{+/+}$ or *S1pr1*$^{-/-}$ myeloid compartment. Scale bars, 20 μm. Left lower panel, CD11b$^+$ myeloid cell clusters were analyzed by confocal microscopy. Scale bars, 100 μm. Right panel, bar graph indicates number of lung nodules from mice with *S1pr1*$^{+/+}$ and *S1pr1*$^{-/-}$ myeloid compartment (n = 6).

Results represent means ± SEM. *p < 0.05, **p < 0.01, ***p < 0.001.

See also Figure S2.

expression and Stat3 activity in the lungs of *Mx1Cre-S1pr1*$^{loxp/loxp}$ mice was accompanied by drastically reduced lung metastasis (Figure 2C, right). Collectively, these data suggest that S1pr1-Stat3 signaling in myeloid cells contributes to premetastatic niche formation, and extensive Stat3 activation in the lung, as well as tumor metastasis. We further analyzed the effects of *S1pr1 and Stat3* ablation on subtypes of CD11b$^+$ cells, such as M1 and M2, as well as N1 and N2, derived from the lung premetastatic sites (Figures S2B and S2C). Moreover, lack of Stat3 in myeloid cells did not significantly change the percentage of myeloid cells in bone marrow and spleen (Figure S2D). T cell subsets were affected by *Stat3* ablation in myeloid compartment at premetastatic niche sites (Figures S2E and S2F). Ablating *Stat3* in myeloid cells also increased T cell proliferation (Figures S2G and S2H).

Targeting S1PR1 or STAT3 in Myeloid Cells Reduces Preformed Metastatic Niches

For potential clinical translation of our results that S1PR1-STAT3 in myeloid cells is critical for premetastatic niche formation, we assessed whether in vivo targeting of *Stat3* or *S1pr1* in myeloid compartment by CpG-*Stat3* siRNA and CpG-*S1pr1* siRNA would effectively reduce preformed metastatic niches at distant organs and thereby prevent metastasis. CpG is a small oligonucleotide with methylated CpG dinucleotides that activate Toll-like receptor (TLR)-9, which is mainly expressed in the endosomal compartment of myeloid and B cells (Kortylewski et al., 2009b). CpG-siRNA can facilitate specific gene silencing in these cells in vivo (Kortylewski et al., 2009b). We first induced premetastatic niches using TCM from *S1pr1*^{high} B16 tumor cells, followed by parental tumor cell injection. The level of *S1pr1* expression was elevated in lungs of mice treated with TCM relative to lungs from control naive mice (Figure S3A). After myeloid cell cluster formation in the lung, mice were treated with CpG-*S1pr1* siRNA. We collected the lungs and analyzed CD11b$^+$ myeloid cells by immunofluorescence staining 3 days after the last CpG-*S1pr1* siRNA treatment. In control CpG-*Luciferase* siRNA-treated mice, we observed abundant myeloid cell infiltration near the distal alveoli (Figure 3A, left), which are the common sites for cell infiltration and metastatic niche formation (Kaplan et al., 2005). In the CpG-*S1pr1* siRNA treatment group, myeloid cell infiltration and cluster formation were drastically reduced compared to those treated with control CpG-*Luciferase* siRNA (Figure 3A). S1pr1 expression in the whole lung was reduced in the CpG-*S1pr1* siRNA-treated group relative to controls (Figure 3B, left). The number of lung metastatic nodules was also greatly reduced by treatment with CpG-*S1pr1* siRNA (Figure 3B, right). We also performed similar experiments with CpG-*Stat3* siRNA to test whether blocking *Stat3* in myeloid cells would reduce preformed premetastatic niches and tumor metastasis. Directly targeting Stat3 in myeloid by CpG-*Stat3* siRNA further reduced tumor factor-induced lung metastasis (Figure 3C). The control CpG-*Luciferase* siRNA treatment also led to somewhat a decrease in lung metastasis compared to PBS treatment, which is likely due to the immune stimulatory effect of CpG (Kortylewski et al., 2009b). We also used inducible genetic ablation of *Stat3* in myeloid cells to confirm that targeting Stat3 in myeloid cells can eliminate pre-existing metastatic niches and metastasis (Figure S3B). CpG-*Stat3* siRNA was also able to eliminate premetastatic that were already formed in lungs after mice were treated with the TCM derived from *S1pr1*^{high} tumor cells (Figure S3C). To assess whether the maintenance of the premetastatic niche requires ongoing production of tumor factors, we performed experiments in which lung myeloid infiltrates were assessed at various time points after treatments with tumor conditioned media was stopped. Data generated from this set of experiments suggest that ongoing production of tumor factors is crucial for the maintenance of the myeloid cell infiltrates in the premetastatic niches (Figure 3D).

STAT3 Signaling Enables Myeloid Cell Invasion and Priming of Premetastatic Sites

Initiation of metastasis involves intravasation of tumor stromal cells, including myeloid cells, from primary tumor sites (Fidler, 2003). We determined whether increasing STAT3 activity intrinsic to myeloid cells could promote their intravasation capacity from primary tumor. We visualized, by multiphoton live imaging, interaction of myeloid cells with tumor endothelium, as a result of increasing Stat3 activity by *S1pr1*^{high} myeloid cells (Figure 4A; Figures S4A and S4B). To further validate that Stat3 activity is crucial for myeloid cells to intravasate at primary tumors, we performed time-lapsed two-photon imaging (Movies S1, S2, S3, and S4), as well as trans-endothelial migration assays with CD11b$^+$ and CD11b$^+$Gr1$^+$ myeloid cells (Figure 4B).

Recent studies emphasize the importance of tumor-secreted factors for premetastatic niche formation (Erler et al., 2009; Hiratsuka et al., 2006; Kim et al., 2009). We next addressed whether myeloid cells, through the S1PR1-STAT3 signaling axis, could also produce factors to condition future metastatic sites. We treated MEFs and primary lung-derived fibroblasts with conditioned media from control and *S1pr1*^{high} myeloid cells and found that both p-Stat3 and fibronectin protein level were higher in fibroblasts treated with conditioned medium from *S1pr1*^{high} myeloid cells compared to those treated with control conditioned medium (Figure 4C). We also detected elevated expression of IL-6, IL-10, and S1P by *S1pr1*^{high} myeloid cells (Figure S4C). In addition, *S1pr1*^{high} myeloid cells mediated increased metastasis (Figure S4D) and produced elevated *Vegf* and *Hif-1*α mRNA and secreted VEGF levels (Figure 4D).

Expression of the receptor for fibronectin, integrin $\alpha_4\beta_1$, by VEGFR1$^+$ myeloid cells has been demonstrated to be critical for premetastatic niche formation (Kaplan et al., 2005). We therefore asked the question whether integrin $\alpha_4\beta_1$ and fibronectin are regulated by Stat3. Real-time PCR revealed that myeloid cells express *Fibronectin* (also known as *Fn1*) in a Stat3-dependent manner (Figure 5A). Tumor cell-produced lysyl oxidase (LOX) has recently been shown to be critical for premetastatic formation (Erler et al., 2009). Real-time PCR analysis indicated that Stat3 could upregulate *Lox* expression in myeloid cells (Figure 5A). We identified STAT-binding sites in the promoter regions of *ITGA4* (encoding integrin α_4), *Fibronectin*, and *LOX* using Transfec. Moreover, chromatin immunoprecipitation (ChIP) assays using chromatins prepared from bone marrow-derived macrophages (BMDMs) exposed to *S1pr1*^{high} TCM indicated that Stat3 protein can directly bind to these sites, suggesting that *Itga4*, *Fibronectin*, and *Lox* are Stat3-target genes, at least in mouse cells (Figure 5B; Figure S5A).

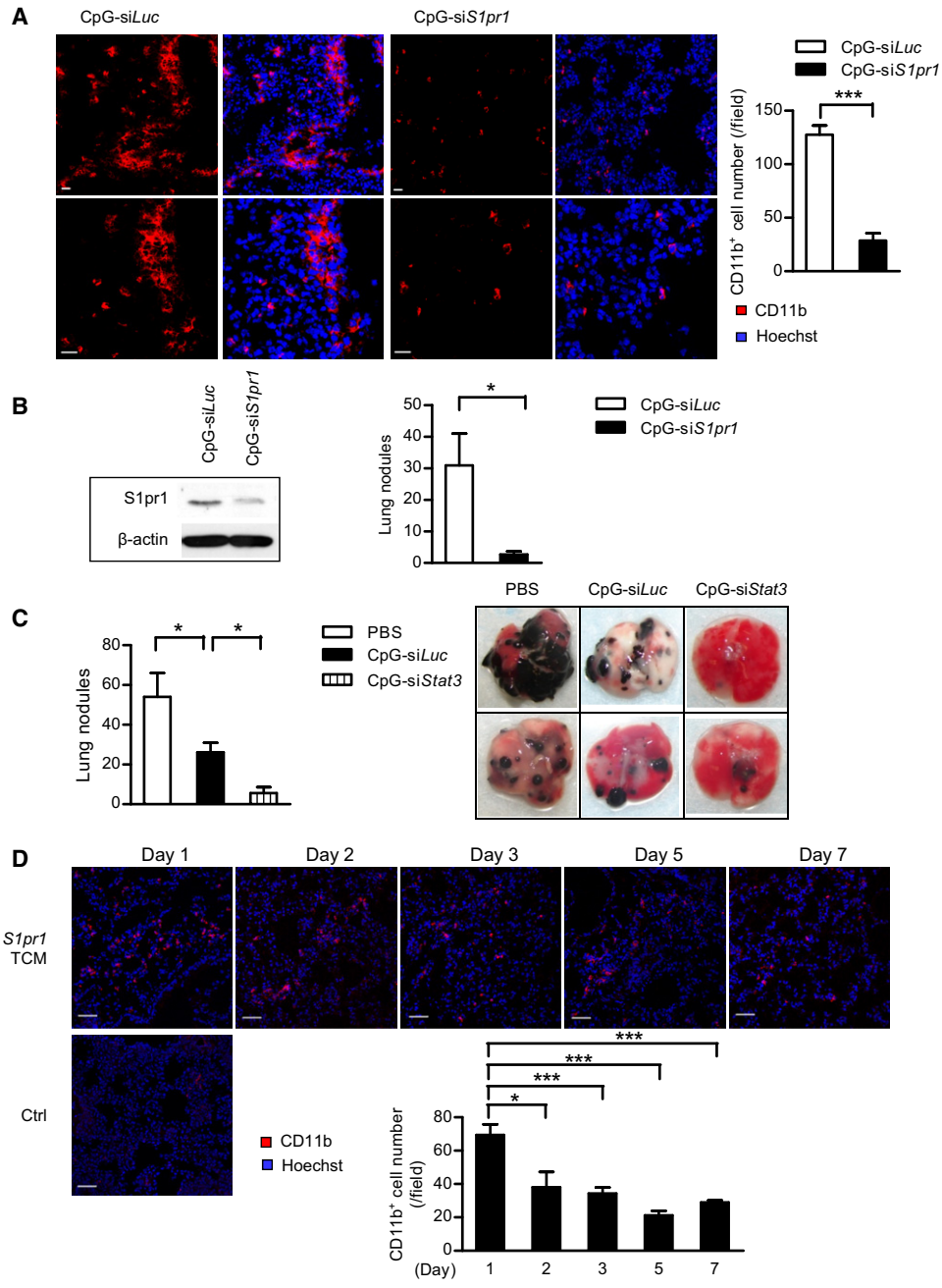

Figure 3. Targeting S1PR1 and STAT3 in Myeloid Cells Can Eliminate Preformed Metastatic Niches

(A) Immunofluorescence staining showing lung myeloid cell infiltrates in mice receiving indicated CpG-siRNA treatments. Left panel: representative images from each group. The images in the lower panel show magnification of upper row of images. Red, $CD11b^+$ myeloid cells; blue, Hoechst staining for nuclei. Right panel: quantification of images on left (n = 8). Scale bars, 20 μm.

(B) Left panel, western blotting measuring effects of CpG-*S1pr1* siRNA on S1pr1 protein expression levels in whole lungs. Right panel, lung metastasis was enumerated after tumor challenge and CpG-*S1pr1* siRNA treatment; shown are representative results from three experiments (n = 6).

(C) Left panel, lung metastatic colonies were enumerated from mice receiving indicated treatments (n = 5). Right panel, representative photos of lungs harvested from mice treated with indicated CpG-siRNA conjugates.

(D) Lung-infiltrating $CD11b^+$ cells were assessed by confocal microscopy. Mice were treated with $S1pr1^{high}$ TCM for 5 days. Upper panel, IF staining of $CD11b^+$ cells in mouse lung tissues harvested at indicated time points after cessation of treatments. Lower left panel, IF staining of $CD11b^+$ cells in a control mouse lung. Scale bars, 50 μm. Lower right panel, quantification of lung infiltrating $CD11b^+$ cells in upper panel (n = 4).

Results represent means ± SEM. *$p < 0.05$, ***$p < 0.001$.

See also Figure S3.

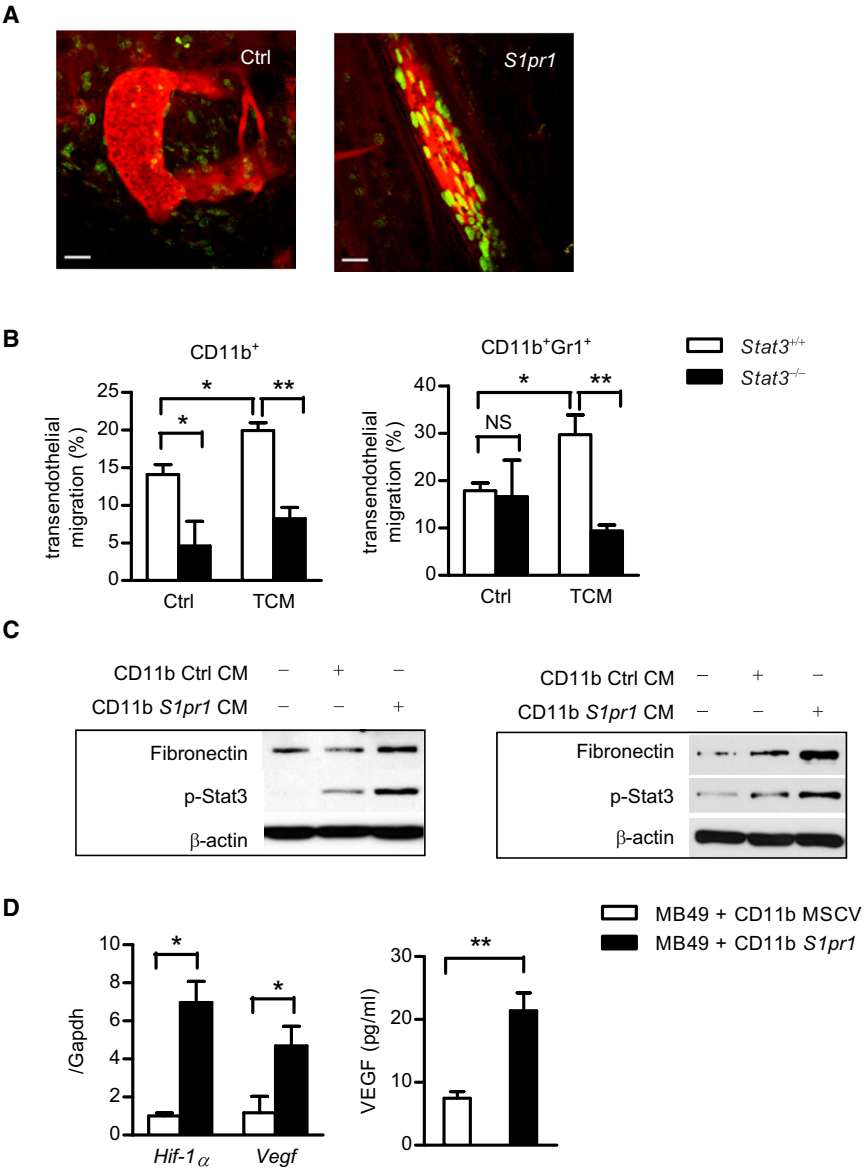

Figure 4. STAT3 in Myeloid Cells Increases Self Invasion and Tumor Metastasis

(A) Intravital two-photon live imaging of primary tumors, visualizing myeloid cell interaction with tumor endothelium. Green, $CD11b^+$ myeloid cells transduced with either *S1pr1* expressing retrovirus or control retrovirus vector with eGFP tag; Red, blood vessels labeled with rhodamine-dextran. Scale bars, 100 μm.

(B) Trans-endothelial migration assay of $Stat3^{+/+}$ and $Stat3^{-/-}$ myeloid cells to migrate across endothelial cells in response to $S1pr1^{high}$ TCM. Migrated $CD11b^+$ (left panel) and $CD11b^+Gr1^+$ (right panel) myeloid cells were further analyzed by flow cytometry and normalized by input total cell numbers; data represents one of three independent experiments.

(C) Western blotting showing Fibronectin and p-Stat3 proteins in MEFs (left) or primary lung-derived fibroblasts (right) incubated with conditioned media (CM) from myeloid cells with or without *S1pr1* overexpression.

(D) Left panel, real-time PCR analysis of whole tumor mixture showing *Hif-1α* and *Vegf* mRNA expression levels, which is normalized by *Gapdh* expression (n = 8). Right panel, tumor secreted VEGF levels were assessed by ELISA using conditioned medium from whole tumors (n = 10).

Results represent means ± SEM. *$p < 0.05$, **$p < 0.01$.

See also Figure S4 and Movies S1, S2, S3, and S4.

We also evaluated expression levels of several known STAT3-regulated genes involved in invasion and matrix-remodeling, processes critical for premetastatic niche formation (Yu et al., 2009) in the BMDMs. Real-time PCR results confirmed that tumor factors can induce expression of *Cxcl2*, *Cxcl12*, *Cxcr4*, *Mmp2*, *Cox-2* in BMDMs in a Stat3-dependent manner (Figure 5A). Furthermore, we showed that tumor factors from $S1pr1^{high}$ tumor cells induced expression of *Il6*, *Il1β*, *Cxcl2*, *Cxcl12,* and *Mmp2* in lung-infiltrating myeloid cells, which is also Stat3-dependent (Figure S5B).

To determine whether myeloid cell production of these STAT3-dependent factors would impact their expression at metastatic sites, we performed ChIP assay using lung tissues collected from mice with $Stat3^{+/+}$ and $Stat3^{-/-}$ in myeloid compartment, challenged with tumor cells. Without Stat3 in the myeloid compartment, metastatic lungs exhibited lowered levels of p-Stat3 (Figure 5C, right). The lung tissue ChIP assays indicated that Stat3 binds to the promoters of *Lox, Mmp2, Mmp9, Itga4, and Cxcl12* in the metastatic tissues (Figure 5C, left). Taken together, we show that through STAT3, whose persistent activation is contributed by S1PR1 in the tumor microenvironment, myeloid cells can express multiple key factors for various aspects of premetastatic niche formation, allowing them to prime the microenvironment at future metastatic sites for their own settlement.

S1PR1-STAT3 Signaling Enables Myeloid Cells to Colonize at Premetastatic Sites

While invasion potential is critical for myeloid cells to colonize/form premetastatic niches at distal organs, myeloid cells must proliferate and evade apoptosis. We therefore assessed whether STAT3 signaling could upregulate expression of prosurvival and proproliferative genes in myeloid cells. Real-time PCR analysis indicated that expression of several prosurvival and proproliferative genes in BMDMs in response to tumor factors was Stat3 dependent (Figure 5A). Expression of the antiproliferative and proapoptotic gene, p53 (Niu et al., 2005), was inhibited by Stat3 in myeloid cells when exposed to the tumor milieu (Figure 5A). To test whether S1PR1-STAT3 signaling in myeloid cells leads to increased proliferation in future metastatic sites, we

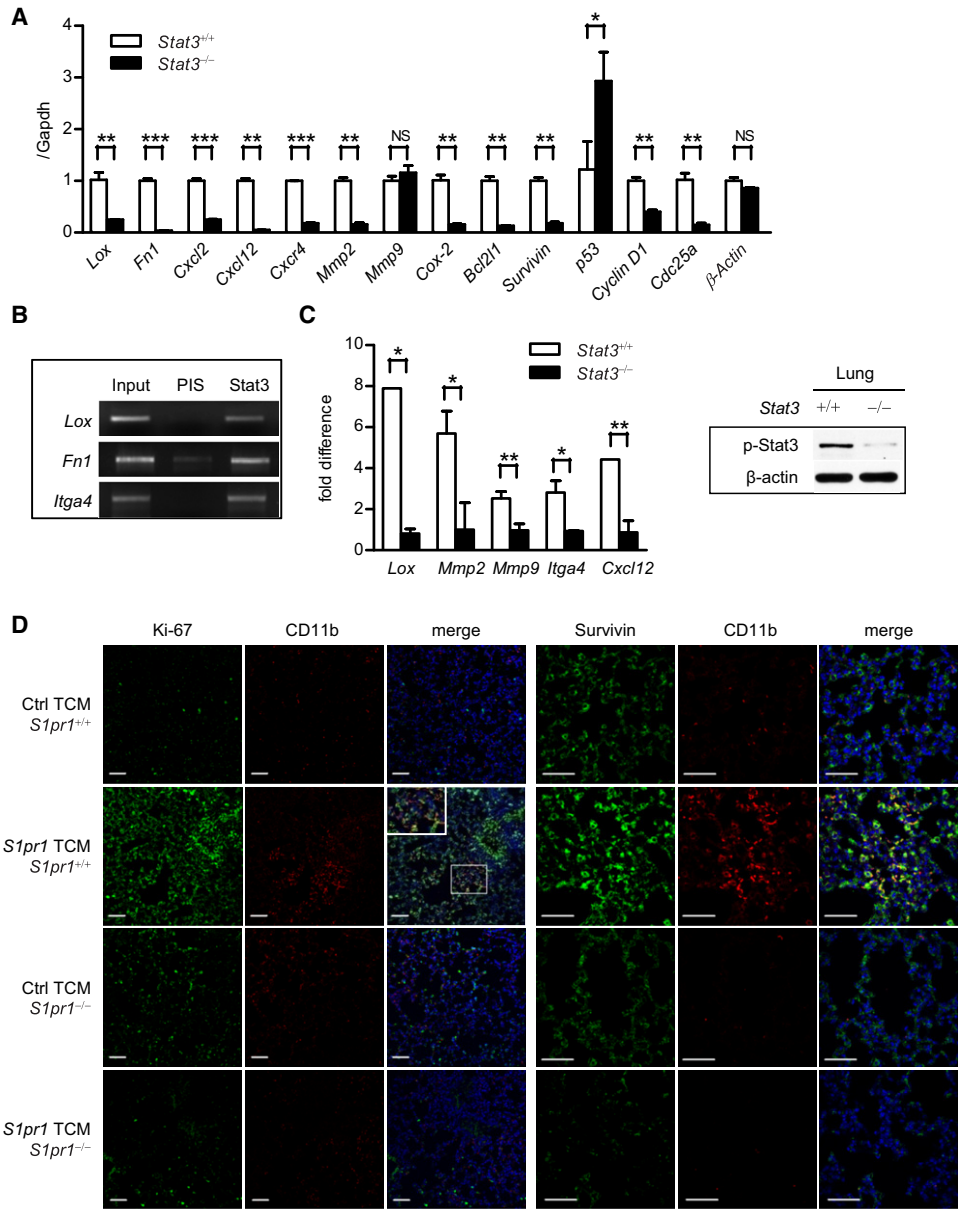

Figure 5. STAT3 Signaling Facilitates Myeloid Cell Colonization

(A) Real-time PCR showing Stat3-dependent expression of indicated genes in *Stat3*$^{+/+}$ and *Stat3*$^{-/-}$ bone marrow-derived macrophages (BMDMs) exposed to TCM (n = 3).

(B) ChIP using BMDMs showing *Itga4*, *Fibronectin* and *Lox* are direct Stat3 target genes. DNA electrophoresis shows DNA fragments within the indicated promoters detected by specific primers. PIS (preimmune serum) antibody was used for immunoprecipitation as a negative control (n = 10).

(C) In vivo ChIP assay of lung tissues collected from mice with *Stat3*$^{+/+}$ or *Stat3*$^{-/-}$ myeloid compartment treated with TCM prior to tumor cell challenge. All ChIP data were quantified by real-time PCR in comparison with input DNA, and normalized with *Stat3*$^{-/-}$ samples set as one. ChIP assay performed in triplicate.

(D) Left panels: double immunofluorescence staining with proliferation marker Ki-67 and myeloid cells marker CD11b, of lung tissue sections prepared from mice with *S1pr1*$^{+/+}$ or *S1pr1*$^{-/-}$ myeloid compartment and treated with indicated TCMs. Inset shows magnification at specified region. Right panels: immunofluorescence staining for detection of Survivin and CD11b in the lungs of indicated mice. Scale bars, 50 μm.

Results represent means ± SEM. *p < 0.05, **p < 0.01, ***p < 0.001.

See also Figure S5.

assessed proliferation index (Ki-67) in the lungs of mice following systemic treatment with *S1pr1*^{high} TCM and found that tumor-derived soluble factors could promote proliferation of cells in premetastatic niches but it depended on S1pr1-Stat3 in the myeloid compartment (Figure 5D, left panels). Notably, the increase in cell proliferation in the premetastatic sites was not restricted to myeloid cells, which was consistent with Stat3 activation in various cells in addition to the myeloid clusters (Figure 1;

Figure S1). We further showed that factors from *S1pr1*^{high} tumors cells induced Stat3-dependent expression of prosurvival/proliferation genes in lung-infiltrating myeloid cells (Figure S5B).

In order to colonize distant sites, myeloid cells must also be able to evade apoptosis in the hostile environment of distant organs. We therefore determined anti-apoptotic gene *Survivin* expression in lung tissue sections adjacent to those used for proliferation analysis. Our results indicated a significant increase in the number of Survivin-positive cells in lungs harvested from mice treated with *S1pr1*^{high} TCM (Figure 5D, right panels). Ablating *S1pr1* in the myeloid compartment abrogated Survivin induction by TCM (Figure 5D, right panels). Consistent with this, we observed Stat3-dependent *Survivin* expression in BMDMs exposed to TCM (Figure 5A).

STAT3 Signaling and Effects in Premetastatic Human Patient Tissues

To extend our findings to human cancers, we analyzed S1PR1 expression and STAT3 activity in uninvolved (tumor cell-free) lymph nodes from high-risk prostate cancer patients and melanoma patients, and from individual without malignancy. We were able to detect strong STAT3 activation in the primary tumor sites (data not shown), and heavy CD68$^+$ myeloid infiltrates in 40 out of 50 uninvolved lymph nodes from the prostate cancer patients, and four out of five uninvolved lymph nodes from the melanoma patients (Figure 6A). CD68$^+$ areas in the lymph nodes also displayed elevated S1PR1 expression and p-STAT3 (Figure 6A). Immunohistochemical staining with another myeloid cells marker, CD33, showed a similar staining pattern as CD68 (Figure S6A). As in mouse premetastatic sites, cells other than myeloid cells including those in the endothelium, also showed increased S1PR1 expression and p-STAT3 levels (Figure S6B). Similar to a prior report (Kaplan et al., 2005), we did not observe heavy CD68$^+$ myeloid infiltrates in the lymph node sections from individual without cancer (Figure 6A). Only weak S1PR1 and p-STAT3 was detected inside normal control lymph nodes (Figure 6A). We further tested SURVIVIN expression in lymph nodes from individuals with prostate cancer and without cancer (Figure 6B, left panel). Quantification of relative expression levels of CD68 and SURVIVIN in the patient lymph nodes versus normal lymph node is also shown (Figure S6C). Expression of BCL2L1 in uninvolved lymph nodes from melanoma patients was associated with elevated p-STAT3 (Figure 6B, right panel).

DISCUSSION

Recent studies suggest a paradigm-shifting concept that non-neoplastic cell populations, such as myeloid cells, are crucial in providing tumor cells a conducive microenvironment to engraft and colonize in distant organs (Erler et al., 2009; Hiratsuka et al., 2006; Kaplan et al., 2005; Kim et al., 2009; Kowanetz et al., 2010; Psaila and Lyden, 2009). This current study introduces the concept that persistent activation of STAT3 occurs in distant organs before tumor cell arrival. *Stat3* or *S1pr1* ablation in myeloid cells also abrogated Stat3 activity in the entire future metastatic site, further suggesting an important role of myeloid cells in establishing premetastatic niches. While induced ablation in the Mx-Cre mice also, to a lesser degree, affects other types of cells in addition to hematopoietic cells, results from CpG-siRNA treatments, which selectively targeting TLR-9$^+$ cells (Kortylewski et al., 2009a, 2009b), support the notion that targeting STAT3/S1PR1 signaling in immune cells can reduce STAT3 activity and myeloid cell infiltrates in future metastatic sites. Consistent with previous studies (Erler et al., 2009; Kaplan et al., 2005; Kim et al., 2009), we show that tumor cell-produced factors, whose upregulation is contributed by S1PR1-STAT3 signaling, are critical in initiating premetastatic niche formation. Our results further indicate that the maintenance of the niche requires ongoing production of tumor factors, suggesting if the tumors are removed timely and completely there would not be premetastatic niches for therapeutic intervention. However, many patients cannot have their tumors removed timely and/or completely, causing relapses. Therefore, targeting premetastatic niches to prevent/reduce metastasis in these patients can be highly desirable. We show that S1PR1-STAT3 signaling-induced tumor factors can prime/activate fibroblasts, which are crucial for forming premetastatic niches at distant organs. These results, taken together, suggest a critical role of S1PR1-STAT3 not only in tumor cells, but also in myeloid cells, and likely in other types of stromal cells including fibroblasts and endothelial cells, in orchestrating premetastatic niche formation.

The focus on initiating distant organ metastasis through myeloid cells has been on tumor cell-produced factors (Erler et al., 2009; Kaplan et al., 2005; Kim et al., 2009). Our data suggest that once STAT3 is persistently activated, myeloid cells produce similar factors as tumor cells, including IL-6 and IL-10, capable of activating fibroblasts and upregulating key molecules, such as fibronectin (Kaplan et al., 2005; Kenny et al., 2008), for premetastatic niche formation. Being able to express integrins and produce chemokines, growth factors, angiogenic factors, and inflammatory mediators in response to tumor factors, is viewed as the primary function of myeloid cells in forming premetastatic niches (Psaila and Lyden, 2009). While these factors/molecules clearly play an important role in premetastatic niche formation, to achieve outgrowth in the hostile environment of distant organs, nonneoplastic cells must sustain proliferation and resist apoptosis. Our results suggest that persistent STAT3 signaling in myeloid cells can increase their proliferation and survival, as well as that of other stromal cells at future metastatic sites. It was previously reported that ablating Stat3 in myeloid cells could enhance the development and progression of colorectal cancer, presumably through inhibition of IL-10 signaling (Deng et al., 2010). In other colorectal cancer models, however, blocking Stat3 was associated with a decrease in tumor development/progression due to inhibition of Th17 (Wu et al., 2009). These results suggest the complexity of immunoregulation in colon cancer, which is greatly impacted by STAT3. At the same time, in many cancers, the role of STAT3 in promoting cancer development and progression has been demonstrated (Yu et al., 2009).

Prior publications suggest that myeloid cells migrate into distant organs from bone marrow without necessarily passing through the primary tumor site (Erler et al., 2009). Our data indicate that S1PR1-STAT3 upregulation in myeloid cells at primary tumor sites can promote their intravasation, which might facilitate their accumulation in future metastatic sites. Activation of Toll-like receptors, specifically TLR2, on myeloid cells by

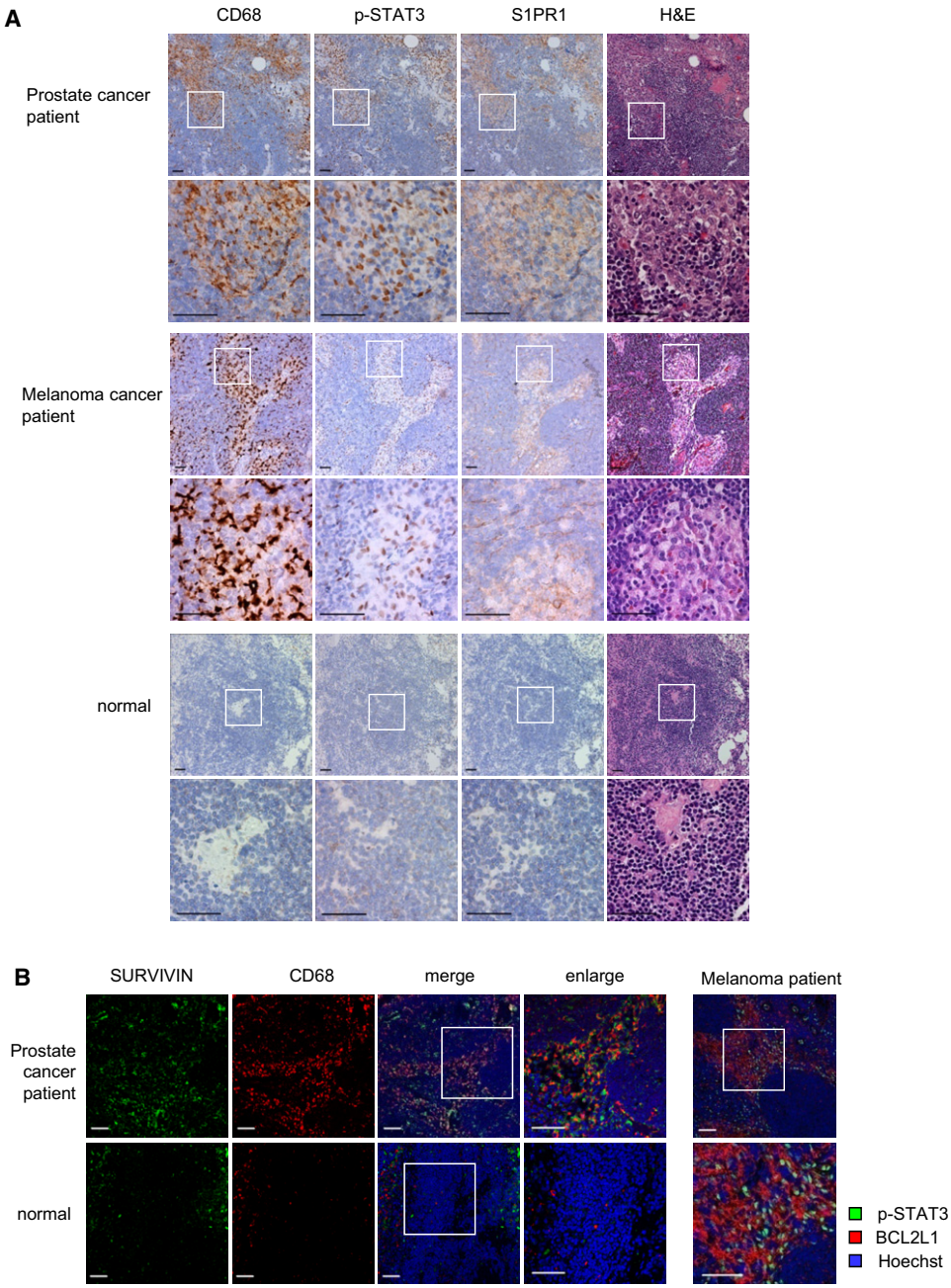

Figure 6. STAT3 Is Activated in Myeloid Clusters in Human Premetastatic Sites

(A) IHC staining of p-STAT3, S1PR1, and CD68 from uninvolved lymph nodes from prostate and melanoma cancer patients with high metastatic potential (upper and middle panels, respectively) or from a control lymph node from an individual without cancer (lower panels).

(B) Immunofluorescence staining from adjacent sections of the same tissues as in (A). Left panel, green, SURVIVIN; red, CD68 of human myeloid cells; blue, nuclei stained with Hoechst. Data on prostate cancer patient lymph nodes are representative of 15 independent patient samples. Right panel, uninvolved lymph nodes from melanoma patients are stained for p-STAT3 (green) and BCL2L1 (red). Nuclei counter stained with Hoechst (blue).

Data are representative of samples from five melanoma patients. Scale bars, 50 μm.

See also Figure S6.

tumor-produced factors has been shown to create an inflammatory milieu that mediates distant-site metastasis (Kim et al., 2009). Because STAT3 can be activated by many inflammatory stimuli through various receptors including Toll-like receptors, and by smoking, carcinogen, radiation, and UV exposure, among other external insults (Arredondo et al., 2006; Aziz et al., 2007; Biswas and Mantovani, 2010; Bronte-Tinkew et al., 2009; Chan et al., 2004; Psaila and Lyden, 2009; Wels et al., 2008; Yu et al., 2009), our findings support the concept that environmental conditions may contribute to cancer metastasis.

Metastasis remains the final frontier for cancer therapy (Klein, 2009; Psaila and Lyden, 2009; Steeg, 2006; Wels et al., 2008). Being able to prevent metastasis by eliminating premetastatic niches is an attractive approach for effective cancer treatment. Our study suggests that the S1PR1-STAT3 axis is operative in not only tumor cells, but also myeloid cells, and likely other types of stromal cells crucially involved in forming premetastatic niches. Our data further expand the STAT3-regulated downstream genes involved in premetastatic niche formation. These studies demonstrate that S1PR1-STAT3 is an effective target to disable both tumor cells and "nonneoplastic" cells from creating an environment that is crucial for malignant distant outgrowth.

EXPERIMENTAL PROCEDURES

Tumor and Myeloid Conditioned Media Preparation

Tumor cells (B16, MB49) were transduced with MSCV retrovirus with or without *S1pr1*. Control and *S1pr1* overexpressing tumor cell lines were incubated in serum-free medium for 24 hr and TCM was collected and filtered through 0.22 μm SFCA membrane (Corning, Inc.). To obtain myeloid cell conditioned media, total splenocytes were harvested and transduced with *S1pr1*-expressing GFP-tagged retrovirus. GFP^+CD11b^+ myeloid cells were FACS sorted after a 24 hr infection, and supernatant was collected 24 hr after culture in RPMI medium supplied with 10% FBS. The supernatants were centrifuged at 3,000 rpm for 5 min.

In Vivo Experiments

Mouse care and experimental procedures were performed in accordance with established institutional guidance and approved protocols from Institutional Animal Care and Use Committee at Beckman Research Institute of City of Hope National Medical Center. We obtained *Mx1-Cre* mice from Jackson Laboratory and $Stat3^{loxp/loxp}$ mice from Drs. Shizuo Akira and Kiyoshi Takeda (Osaka University). $Stat3^{-/-}$ ablation in hematopoietic cells was accomplished as previously described (Kortylewski et al., 2005). $S1pr1^{loxp/loxp}$ mice (generous gift from Dr. Richard Proia) were crossed with *Mx1-Cre* mice to generate *S1pr1* deletion in hematopoietic cells as previously described (Lee et al., 2010).

For TCM treatments, mice were treated by intraperitoneal injection of TCM (300 μl) followed by parental tumor cell tail vein injection (1×10^5/mouse). Lungs were perfused using HBSS, harvested and immediately embedded in OCT or fixed with formalin.

For tumor cell/myeloid cell co-administration, GFP^+CD11b^+ myeloid cells, transduced and sorted as described above, were mixed with either MB49 or B16 tumor cells (1:10 ratio), and subsequently injected into mice either subcutaneously or through tail vein injection.

CpG conjugated siRNA was synthesized as previously described (Kortylewski et al., 2009b). The sequences of CpG-*Luc* siRNA and CpG-*Stat3* siRNA conjugate molecules were reported elsewhere (Kortylewski et al., 2009b). C57BL/6 mice were treated with TCM for 5 consecutive days, followed by i.v. parental tumor cell challenge. Mice were first treated (i.v.) with CpG-siRNA conjugates (0.78 nmol/mice) at day 7 post-tumor challenge, followed by every other day treatment for 2 weeks. Lungs were perfused, harvested, and embedded in OCT for further analysis.

Immunohistochemistry and Immunofluorescent Staining and Analyses

Paraffin-embedded sections were deparaffinized, followed by staining with antibodies against pY705-Stat3 (Cell Signaling Technology), S1PR1 (Santa Cruz Biotechnology Inc.) or CD68 (AbD Serotec) and examined under Olympus AX70 automated upright microscope. Frozen or deparaffinized sections were stained with pY705-Stat3 (Santa Cruz Biotechnology Inc.), CD11b (BD PharMingen), Ki-67 (Abcam), and Survivin (Novus Biologicals) antibodies. For fluorescence detection, secondary antibodies were used (Alexa Fluor 488 and Alexa Fluor 546, Invitrogen) and counterstained with Hoechst 33432 (Invitrogen) for nuclei. Slides were mounted and examined using the Zeiss cLSM510Meta inverted confocal microscope. Image-Pro Plus (MediaCybernetics) software was used to count the number of stained cells as indicated in the figure legends for quantification purpose.

Intravital Two-Photon Imaging, Time-Lapse 3D Imaging, and Analysis

After injection of tumor cells mixed with myeloid cells (GFP-tagged) for 9 days, mice were retroorbitally injected with dextran-rhodamine (Invitrogen) and were anesthetized 30 min later. Live imaging was performed using Prairie Ultima microscope (Prairie Technologies, Madison, WI) as previously described (Kortylewski et al., 2009b). Both green and red channels were excited at 860 nm, with emission detected simultaneously between 500 and 550 nm (green/GFP) and between 570 and 620 nm (red/Dextran). Multidimensional images were created as previously reported (Wei et al., 2005), Z-stack images were acquired (20x/1.0W objective by Olympus, 1024 × 1024 = 0.464 μm/pixel) every 5 min for 13 time points to create a 4D data set (x, y, and z axes with time and different emission wavelengths). Fourteen Z-sections were collected at 3 μm intervals for a total of 42 μm. Z-stacks images were first assembled in Image Pro Plus software version 6.3 (Media Cybernetics), and then 3D data sets were generated using Amira software version 5.3.3 (Visage Imaging) using Volren projections. Time-lapse sequences were created using Amira Demo Maker and Movie Maker. Movies were saved in the MPG format with 200 frames at a rate of 24 fps.

Trans-Endothelial Migration Assay

Mouse prostate endothelial cells were seeded in 24-well transwell inserts (Corning Costar Corp.) with polycarbonate membranes (8.0 μm pore). For trans-endothelial cell migration, myeloid cells were stained with CD11b and Gr1 antibodies and re-suspended in leukocyte migration buffer containing RPMI 1640 medium with 0.25% BSA (fatty acid free, Sigma), and added to the upper chamber at 1×10^5/well. Cells were allowed to migrate toward TCM in lower chamber for 1 hr. The numbers of migrated cells into lower chamber were enumerated for different myeloid subpopulations by flow cytometry at a fixed flow rate for 1 min on Accuri C6 flow cytometer. The percentage of migrated cells was normalized by the total numbers of input cells for each sample.

Chromatin Immunoprecipitation Assay

ChIP assays for cells and tissues were performed based on the protocol from Millipore-Upstate Biotechnology. Rabbit anti-Stat3 (C-20, Santa Cruz Biotechnology, Inc.) was used for immunoprecipitation. Potential STAT-binding sites on mouse *Lox*, *Fibronectin, Vla-4*, *Mmp2* and *Mmp9* were analyzed by Transfec software. The potential Stat binding sites are: *Lox* (5′-TTCCCATAA-3′, −405 bp); *Fibronectin* (5′-TTCCCACAA-3′, −574 bp); *Itga4* (5′-TTCCCCCAA-3′, −229 bp); *Mmp2* (5′-TTCCTGGAA-3′, −1,667 bp); *Mmp9* (5′-TTCCCCAA-3′, −579 bp). ChIP primers were designed to flank these sites: for *Lox,* 5′-CGTAGCAAGCTTTGTTCCCT-3′, 5′-GGGAGGTTGTGACTA AGGCTTATGCT-3′; *Fibronectin*, 5′-AAACCGAGGTCTGAGCCTACCTAA-3′, 5′- AATTGGTGGCTGTGGTGGTGTTTG-3′; *Itga4*, 5′-CCCAAATTATTGGCC ACTGGGACT-3′, 5′- ACCTAGGTTGCATGGACTCACA-3′; *Mmp2*, 5′-ATTG GCAGGCCCATTTGGGTTGAT-3′, 5′-TCAGGGATTCACGGTTGTCACCTT-3′, *Mmp9*, 5′-ATAGGGACAAAGGCTTGAGCGACA-3′, 5′- AGCAGGCTCTTTGA GGCAGGATTT-3′. *Cxcl12* primer was used according to previous publication (Stat3 biding site 5′-TTCCCGGGAA-3′, −527 bp) (Olive et al., 2008), 5′-ACCTGTTTGGTCTCTTTGCTCGGT-3′, 5′-CTGTCAAAGGCACAAGCCGTGA AA-3′. The relative amount of precipitated DNAs were quantified by real-time PCR and normalized by input DNA.

Patient and Normal Lymph Node Specimens

Prostate cancer patient specimens were obtained through a City of Hope Institutional Review Board approved protocol (COH IRB 09213) with consent from patients. Briefly, 50 high-risk prostate cancer patients (defined by standard D'Amico criteria, i.e., baseline PSA >20 ng/m, Gleason grade 8–10, or stage T3a-T4 disease), who were treated with prostatectomy, were selected. Paraffin-embedded tissue from benign pelvic lymph nodes were obtained and prepared as 4 μm sections on unstained slides for subsequent analyses. Lymph node sections from melanoma were prepared for immunohistochemistry (IHC) analysis as previously described (de Maat et al., 2007), and were

provided by John Wayne Cancer Institute, with approval from Western Institutional Review Board and with patient consent. Lymph node tissue sections from individuals without cancer were purchased from Abcam. Tissue sections were stained and examined as described above. Paraffin-embedded tissue slides were stained with H&E and examined/diagnosed by a licensed pathologist.

Statistics

Data are presented as means ± SEM. Statistical comparisons between groups were performed using unpaired Student's t tests to calculate the two-tailed p value: *p < 0.05, **p < 0.01, ***p < 0.001.

SUPPLEMENTAL INFORMATION

Supplemental Information includes six figures, Supplemental Experimental Procedures, and four movies and can be found with this article online at doi:10.1016/j.ccr.2012.03.039.

ACKNOWLEDGMENTS

We would like to thank Dr. Brian Armstrong and other staff members of Light Microscopy Imaging Core, and Dr Bogdan Gabriel Gugiu at Mass Spectrometry and Proteomics Core, at Beckman Research Institute, City of Hope Comprehensive Cancer Center, for time-lapsed imaging and for measuring S1P, respectively. We are also grateful to staff members at Pathology Core, Flow Cytometry Core and Animal Facility Core at City of Hope for technical assistance. We would also like to thank Dr. Richard Proia (US National Institute of Health) for providing *S1pr1*$^{loxp/loxp}$ mice, Dr. Edouard Cantin at City of Hope for providing L929 cell line, Piotr Swiderski at City of Hope for CpG-siRNA construct synthesis. This work is funded by Markel fund and Tim Nesviq Fund at City of Hope Comprehensive Cancer Center, Keck Foundation and R01 CA115815, R01 CA122976 and R01 CA115674, P30 CA33572 from the NCI, as well as National Natural Science Foundation Grants of China (91129702, 81125001). Procurement of patient samples and normal lymph nodes were supported by NIH grant 2K12CA001727-16A1 and Abcam.

Received: April 21, 2011
Revised: November 28, 2011
Accepted: March 5, 2012
Published: May 14, 2012

REFERENCES

Arredondo, J., Chernyavsky, A.I., Jolkovsky, D.L., Pinkerton, K.E., and Grando, S.A. (2006). Receptor-mediated tobacco toxicity: cooperation of the Ras/Raf-1/MEK1/ERK and JAK-2/STAT-3 pathways downstream of alpha7 nicotinic receptor in oral keratinocytes. FASEB J. *20*, 2093–2101.

Aziz, M.H., Manoharan, H.T., and Verma, A.K. (2007). Protein kinase C epsilon, which sensitizes skin to sun's UV radiation-induced cutaneous damage and development of squamous cell carcinomas, associates with Stat3. Cancer Res. *67*, 1385–1394.

Biswas, S.K., and Mantovani, A. (2010). Macrophage plasticity and interaction with lymphocyte subsets: cancer as a paradigm. Nat. Immunol. *11*, 889–896.

Bollrath, J., Phesse, T.J., von Burstin, V.A., Putoczki, T., Bennecke, M., Bateman, T., Nebelsiek, T., Lundgren-May, T., Canli, O., Schwitalla, S., et al. (2009). gp130-mediated Stat3 activation in enterocytes regulates cell survival and cell-cycle progression during colitis-associated tumorigenesis. Cancer Cell *15*, 91–102.

Bromberg, J.F., Wrzeszczynska, M.H., Devgan, G., Zhao, Y., Pestell, R.G., Albanese, C., and Darnell, J.E., Jr. (1999). Stat3 as an oncogene. Cell *98*, 295–303.

Bronte-Tinkew, D.M., Terebiznik, M., Franco, A., Ang, M., Ahn, D., Mimuro, H., Sasakawa, C., Ropeleski, M.J., Peek, R.M., Jr., and Jones, N.L. (2009). Helicobacter pylori cytotoxin-associated gene A activates the signal transducer and activator of transcription 3 pathway in vitro and in vivo. Cancer Res. *69*, 632–639.

Catlett-Falcone, R., Landowski, T.H., Oshiro, M.M., Turkson, J., Levitzki, A., Savino, R., Ciliberto, G., Moscinski, L., Fernández-Luna, J.L., Nuñez, G., et al. (1999). Constitutive activation of Stat3 signaling confers resistance to apoptosis in human U266 myeloma cells. Immunity *10*, 105–115.

Chae, S.S., Paik, J.H., Furneaux, H., and Hla, T. (2004). Requirement for sphingosine 1-phosphate receptor-1 in tumor angiogenesis demonstrated by in vivo RNA interference. J. Clin. Invest. *114*, 1082–1089.

Chan, K.S., Sano, S., Kiguchi, K., Anders, J., Komazawa, N., Takeda, J., and DiGiovanni, J. (2004). Disruption of Stat3 reveals a critical role in both the initiation and the promotion stages of epithelial carcinogenesis. J. Clin. Invest. *114*, 720–728.

Chiarle, R., Simmons, W.J., Cai, H., Dhall, G., Zamo, A., Raz, R., Karras, J.G., Levy, D.E., and Inghirami, G. (2005). Stat3 is required for ALK-mediated lymphomagenesis and provides a possible therapeutic target. Nat. Med. *11*, 623–629.

Coussens, L.M., Tinkle, C.L., Hanahan, D., and Werb, Z. (2000). MMP-9 supplied by bone marrow-derived cells contributes to skin carcinogenesis. Cell *103*, 481–490.

de Maat, M.F., van de Velde, C.J., Umetani, N., de Heer, P., Putter, H., van Hoesel, A.Q., Meijer, G.A., van Grieken, N.C., Kuppen, P.J., Bilchik, A.J., et al. (2007). Epigenetic silencing of cyclooxygenase-2 affects clinical outcome in gastric cancer. J. Clin. Oncol. *25*, 4887–4894.

Deng, L., Zhou, J.F., Sellers, R.S., Li, J.F., Nguyen, A.V., Wang, Y., Orlofsky, A., Liu, Q., Hume, D.A., Pollard, J.W., et al. (2010). A novel mouse model of inflammatory bowel disease links mammalian target of rapamycin-dependent hyperproliferation of colonic epithelium to inflammation-associated tumorigenesis. Am. J. Pathol. *176*, 952–967.

Du, R., Lu, K.V., Petritsch, C., Liu, P., Ganss, R., Passegué, E., Song, H., Vandenberg, S., Johnson, R.S., Werb, Z., and Bergers, G. (2008). HIF1alpha induces the recruitment of bone marrow-derived vascular modulatory cells to regulate tumor angiogenesis and invasion. Cancer Cell *13*, 206–220.

Erler, J.T., Bennewith, K.L., Cox, T.R., Lang, G., Bird, D., Koong, A., Le, Q.T., and Giaccia, A.J. (2009). Hypoxia-induced lysyl oxidase is a critical mediator of bone marrow cell recruitment to form the premetastatic niche. Cancer Cell *15*, 35–44.

Fan, J., and Malik, A.B. (2003). Toll-like receptor-4 (TLR4) signaling augments chemokine-induced neutrophil migration by modulating cell surface expression of chemokine receptors. Nat. Med. *9*, 315–321.

Fidler, I.J. (2003). The pathogenesis of cancer metastasis: the 'seed and soil' hypothesis revisited. Nat. Rev. Cancer *3*, 453–458.

Fukuda, A., Wang, S.C., Morris, J.P., 4th, Folias, A.E., Liou, A., Kim, G.E., Akira, S., Boucher, K.M., Firpo, M.A., Mulvihill, S.J., and Hebrok, M. (2011). Stat3 and MMP7 contribute to pancreatic ductal adenocarcinoma initiation and progression. Cancer Cell *19*, 441–455.

Gao, D., Nolan, D.J., Mellick, A.S., Bambino, K., McDonnell, K., and Mittal, V. (2008). Endothelial progenitor cells control the angiogenic switch in mouse lung metastasis. Science *319*, 195–198.

Grivennikov, S., Karin, E., Terzic, J., Mucida, D., Yu, G.Y., Vallabhapurapu, S., Scheller, J., Rose-John, S., Cheroutre, H., Eckmann, L., and Karin, M. (2009). IL-6 and Stat3 are required for survival of intestinal epithelial cells and development of colitis-associated cancer. Cancer Cell *15*, 103–113.

Hiratsuka, S., Watanabe, A., Aburatani, H., and Maru, Y. (2006). Tumour-mediated upregulation of chemoattractants and recruitment of myeloid cells predetermines lung metastasis. Nat. Cell Biol. *8*, 1369–1375.

Holmgren, L., O'Reilly, M.S., and Folkman, J. (1995). Dormancy of micrometastases: balanced proliferation and apoptosis in the presence of angiogenesis suppression. Nat. Med. *1*, 149–153.

Kaplan, R.N., Riba, R.D., Zacharoulis, S., Bramley, A.H., Vincent, L., Costa, C., MacDonald, D.D., Jin, D.K., Shido, K., Kerns, S.A., et al. (2005). VEGFR1-positive haematopoietic bone marrow progenitors initiate the pre-metastatic niche. Nature *438*, 820–827.

Kenny, H.A., Kaur, S., Coussens, L.M., and Lengyel, E. (2008). The initial steps of ovarian cancer cell metastasis are mediated by MMP-2 cleavage of vitronectin and fibronectin. J. Clin. Invest. *118*, 1367–1379.

Kim, S., Takahashi, H., Lin, W.W., Descargues, P., Grivennikov, S., Kim, Y., Luo, J.L., and Karin, M. (2009). Carcinoma-produced factors activate myeloid cells through TLR2 to stimulate metastasis. Nature *457*, 102–106.

Klein, C.A. (2009). Parallel progression of primary tumours and metastases. Nat. Rev. Cancer *9*, 302–312.

Kortylewski, M., Kujawski, M., Wang, T., Wei, S., Zhang, S., Pilon-Thomas, S., Niu, G., Kay, H., Mulé, J., Kerr, W.G., et al. (2005). Inhibiting Stat3 signaling in the hematopoietic system elicits multicomponent antitumor immunity. Nat. Med. *11*, 1314–1321.

Kortylewski, M., Kujawski, M., Herrmann, A., Yang, C., Wang, L., Liu, Y., Salcedo, R., and Yu, H. (2009a). Toll-like receptor 9 activation of signal transducer and activator of transcription 3 constrains its agonist-based immunotherapy. Cancer Res. *69*, 2497–2505.

Kortylewski, M., Swiderski, P., Herrmann, A., Wang, L., Kowolik, C., Kujawski, M., Lee, H., Scuto, A., Liu, Y., Yang, C., et al. (2009b). In vivo delivery of siRNA to immune cells by conjugation to a TLR9 agonist enhances antitumor immune responses. Nat. Biotechnol. *27*, 925–932.

Kortylewski, M., Xin, H., Kujawski, M., Lee, H., Liu, Y., Harris, T., Drake, C., Pardoll, D., and Yu, H. (2009c). Regulation of the IL-23 and IL-12 balance by Stat3 signaling in the tumor microenvironment. Cancer Cell *15*, 114–123.

Kowanetz, M., Wu, X., Lee, J., Tan, M., Hagenbeek, T., Qu, X., Yu, L., Ross, J., Korsisaari, N., Cao, T., et al. (2010). Granulocyte-colony stimulating factor promotes lung metastasis through mobilization of Ly6G+Ly6C+ granulocytes. Proc. Natl. Acad. Sci. USA *107*, 21248–21255.

Kujawski, M., Kortylewski, M., Lee, H., Herrmann, A., Kay, H., and Yu, H. (2008). Stat3 mediates myeloid cell-dependent tumor angiogenesis in mice. J. Clin. Invest. *118*, 3367–3377.

Lee, H., Deng, J., Kujawski, M., Yang, C., Liu, Y., Herrmann, A., Kortylewski, M., Horne, D., Somlo, G., Forman, S., et al. (2010). STAT3-induced S1PR1 expression is crucial for persistent STAT3 activation in tumors. Nat. Med. *16*, 1421–1428.

Lesina, M., Kurkowski, M.U., Ludes, K., Rose-John, S., Treiber, M., Klöppel, G., Yoshimura, A., Reindl, W., Sipos, B., Akira, S., et al. (2011). Stat3/Socs3 activation by IL-6 transsignaling promotes progression of pancreatic intraepithelial neoplasia and development of pancreatic cancer. Cancer Cell *19*, 456–469.

Mantovani, A., Allavena, P., Sica, A., and Balkwill, F. (2008). Cancer-related inflammation. Nature *454*, 436–444.

Niu, G., Wright, K.L., Ma, Y., Wright, G.M., Huang, M., Irby, R., Briggs, J., Karras, J., Cress, W.D., Pardoll, D., et al. (2005). Role of Stat3 in regulating p53 expression and function. Mol. Cell. Biol. *25*, 7432–7440.

Olive, M., Mellad, J.A., Beltran, L.E., Ma, M., Cimato, T., Noguchi, A.C., San, H., Childs, R., Kovacic, J.C., and Boehm, M. (2008). p21Cip1 modulates arterial wound repair through the stromal cell-derived factor-1/CXCR4 axis in mice. J. Clin. Invest. *118*, 2050–2061.

Orimo, A., Gupta, P.B., Sgroi, D.C., Arenzana-Seisdedos, F., Delaunay, T., Naeem, R., Carey, V.J., Richardson, A.L., and Weinberg, R.A. (2005). Stromal fibroblasts present in invasive human breast carcinomas promote tumor growth and angiogenesis through elevated SDF-1/CXCL12 secretion. Cell *121*, 335–348.

Pollard, J.W. (2004). Tumour-educated macrophages promote tumour progression and metastasis. Nat. Rev. Cancer *4*, 71–78.

Psaila, B., and Lyden, D. (2009). The metastatic niche: adapting the foreign soil. Nat. Rev. Cancer *9*, 285–293.

Shojaei, F., Wu, X., Zhong, C., Yu, L., Liang, X.H., Yao, J., Blanchard, D., Bais, C., Peale, F.V., van Bruggen, N., et al. (2007). Bv8 regulates myeloid-cell-dependent tumour angiogenesis. Nature *450*, 825–831.

Spiegel, S., and Milstien, S. (2003). Sphingosine-1-phosphate: an enigmatic signalling lipid. Nat. Rev. Mol. Cell Biol. *4*, 397–407.

Steeg, P.S. (2006). Tumor metastasis: mechanistic insights and clinical challenges. Nat. Med. *12*, 895–904.

Visentin, B., Vekich, J.A., Sibbald, B.J., Cavalli, A.L., Moreno, K.M., Matteo, R.G., Garland, W.A., Lu, Y., Yu, S., Hall, H.S., et al. (2006). Validation of an anti-sphingosine-1-phosphate antibody as a potential therapeutic in reducing growth, invasion, and angiogenesis in multiple tumor lineages. Cancer Cell *9*, 225–238.

Wang, L., Yi, T., Kortylewski, M., Pardoll, D.M., Zeng, D., and Yu, H. (2009). IL-17 can promote tumor growth through an IL-6-Stat3 signaling pathway. J. Exp. Med. *206*, 1457–1464.

Wei, S.H., Rosen, H., Matheu, M.P., Sanna, M.G., Wang, S.K., Jo, E., Wong, C.H., Parker, I., and Cahalan, M.D. (2005). Sphingosine 1-phosphate type 1 receptor agonism inhibits transendothelial migration of medullary T cells to lymphatic sinuses. Nat. Immunol. *6*, 1228–1235.

Wels, J., Kaplan, R.N., Rafii, S., and Lyden, D. (2008). Migratory neighbors and distant invaders: tumor-associated niche cells. Genes Dev. *22*, 559–574.

Wu, S., Rhee, K.J., Albesiano, E., Rabizadeh, S., Wu, X., Yen, H.R., Huso, D.L., Brancati, F.L., Wick, E., McAllister, F., et al. (2009). A human colonic commensal promotes colon tumorigenesis via activation of T helper type 17 T cell responses. Nat. Med. *15*, 1016–1022.

Yu, H., Kortylewski, M., and Pardoll, D. (2007). Crosstalk between cancer and immune cells: role of STAT3 in the tumour microenvironment. Nat. Rev. Immunol. *7*, 41–51.

Yu, H., Pardoll, D., and Jove, R. (2009). STATs in cancer inflammation and immunity: a leading role for STAT3. Nat. Rev. Cancer *9*, 798–809.